Sustainable Energy Technologies and Assessments 60 (2023) 103404

Contents lists available at ScienceDirect

Sustainable Energy Technologies and Assessments

journal homepage: www.elsevier.com/locate/seta

A flexibility management system for behind-the-meter flexibility with distributed energy resources: A sensitivity analysis

Jose-Fernando Forero-Quintero *, Roberto Villafafila-Robles, Sara Barja-Martinez, Marina Codina-Escolar, Daniel Montesinos-Miracle

Centre d'Innovació Tecnològica en Convertidors Estàtics i Accionaments (CITCEA-UPC), Department d'Enginyeria Elèctrica, Universitat Politècnica de Catalunya, UPC, Av. Diagonal 647, Pl. 2. 08028, Barcelona, Spain

ARTICLE INFO

MSC:
00-01
99-00

Keywords:
Flexibility management system
Energy cost optimization
Cost–benefit analysis

ABSTRACT

The increasing uncertainty in power systems with high penetration levels of renewable energy fosters the research on the control, management, and operation of distributed energy resources and its coupling with the current grid operation and control scheme alongside future energy markets and flexibility services. This work proposes a flexibility management system for the behind-the-meter flexibility of the distributed energy resources, which employs an adaptive auto-regression forecasting module to predict the energy cost overruns of the system throughout the energy exchanges at the point of interconnection. In addition, a cost–benefit analysis is used to evaluate and optimize the DER set-point profiles to minimize the installation's energy cost, which, together with power redispatching and unit recommitment modules, are executed to adjust the DER operating points according to real-time deviations and short-term flexibility requests. A reference case and sensitivity analysis are performed to demonstrate the efficiency of the management system and the influence of relevant parameters. According to the results, the proposed flexibility management system reduces the total energy cost by 45% and 27.8% using quadratic and linear cost function approaches, respectively, with an average calculation time of 236 s per 900 s of execution.

Introduction

The high uncertainty in power systems with a considerable penetration level of renewable energy is impulsing the research on power system flexibility, as a key component of the balancing of the system. [1] studies the generation-side flexibility of integrating variable renewable energy sources in the power system in terms of energy planning, balancing, and investments. From demand-side flexibility, works such as [2,3] measure the flexibility offered by end-users to the distribution grid for diverse ancillary services. All the necessary flexibility throughout the electrical system requires control and management systems capable of guaranteeing a safe, reliable, profitable, and balanced operation of the network, as well as the optimization of energy resources.

To control the behind-the-meter flexibility generated by end-users with Distributed Energy Resources (DER), [4] tested an Energy Management System (EMS) in charge of producing an optimal day-ahead energy scheduling of DER assets (Electric Vehicle (EV) charger, Photovoltaic Panel (PV), and stationary battery) for every 15-min of the day, in which operational boundaries and costs are deemed. Otherwise, [5,6] propose to manage controllable residential appliances to reduce peak demand through voltage control in an hourly energy program. [7] prioritizes the management of photovoltaic production to reduce the electricity consumption cost of consumers, as well as, [8] optimizes the usage, size, and location of the battery banks to minimize the individual electricity bills. [9] attempts to handle PV production and lithium-ion storage batteries in order to optimize the energy cost of the end-user. All these above studies are focusing on particular DERs, individually. With the same objectives, [10] optimally control the power at Point pf Connection (POI) to minimize the electricity bill of the end-user, according to Time-of-Use (ToU) tariffs.

These studies are chiefly concerned with DERs, individually or just the demand at POI. In general, many disturbances, forecast errors, and unexpected events harm the optimal energy schedule, moving it away from its ideal state, failing to comply with expected behavior, and generating cost overruns during real-time operation. A low-level control system is needed to solve these problems and provide short-term flexibility to the grid. Addressing this uncertainty problem, [11] defines a decentralized energy flexibility management in power system distribution, where it formulates the interaction between DSO, end-user, and aggregator to reduce the expected cost of each consumer and

* Corresponding author.
E-mail address: jose.fernando.forero@upc.edu (J.-F. Forero-Quintero).

https://doi.org/10.1016/j.seta.2023.103404
Received 3 April 2023; Received in revised form 24 July 2023; Accepted 10 August 2023
Available online 3 September 2023
2213-1388/© 2023 The Authors. Published by Elsevier Ltd. This is an open access article under the CC BY-NC-ND license (http://creativecommons.org/licenses/by-nc-nd/4.0/).

Nomenclature

ACM	Aging Cost Model
AMI	Advanced Metering Infrastructure
ARA	Adaptive Auto-regression Algorithm
BRP	Balance Responsible Party
CBA	Cost–Benefit Analysis
CO_2	Carbon Dioxide
DER	Distributed Energy Resources
DG	Distributed Generation
DoD	Depth of Discharge
DSO	Distributed System Operator
EMS	Energy Management System
EOL	End-of-life
EV	Electric Vehicle
FLEMS	Flexibility Management System
GA	Genetic Algorithm
O&M	Operation and Maintenance
POI	Point of Interconnection
PV	Photovoltaic Panel
PVPC	Precio Voluntario Pequeño Consumidor
RDM	Redispatching Module
RES	Renewable Energy Sources
RMS	Real-time Management System
SO	System Operator
SoC	State of Charge
TLC	Traffic Line Concept
T&D	Transmission & Distribution
ToU	Time-of-Use
TSO	Transmission System Operator
URM	Unit Recommitment Module

Variables and Parameters

a_c	Quadratic parameter of quadratic cost function
$Ah(c)$	Accumulated ampere-hour throughput at given current c (Ampere-hour)
Ah_t	Total aging effect caused by cycling at time t (Ampere-hour)
$B(c)$	C-rate dependent pre-exponential factor at given current c
c	Independent parameter of quadratic cost function
C_{flex}	Flexibility cost (€)
C_{lcc}	Battery Life Cycle Costs (€/kWh)
Cag_t	Aging cost for cycling at time t (€)
$Clife$	Battery life cycle (Cycles)
Cn_t	Capacity loss at time t (%)
Com_t	Operation and Maintenance cost at time t (€)
$Cred_t$	Cost for reducing active power at time t (€)
Cur_t	Solar curtailment at time t (kW)
Cur_{tol}	Solar curtailment tolerable (kW)
$Ea(c)$	Activation energy at given current c (J/mol)
Ech_t	Energy charged at time t (kW)
$Edis_t$	Energy discharged at time t (kW)
Ik_t	Measured current at time t (Ampere)
$Inom$	Nominal charging and discharging current (Ampere)
$Kag^{ESS}_{t,SOC}$	Aging factor in terms of the average SOC of each cycle
N	Power ramp rate period (hour)
$Nk(c,Ta)$	Number of cycles before EOL at given current c and Ta (Cycles
$Npos^{ESS}_{t,DOD}$	Maximum of the possible cycles in a battery life time to the given DoD level (Cycles)
P_{min}	Minimum active power (kW)
P_{nom}	Rated active power (kW)
P_t	Active power at time t (kW)
Pch_{max}	Maximum power for charging at time N (kW)
$Pdis_{max}$	Maximum power for discharging at time N (kW)
$Ppoi_t$	Measured active power at POI at time t (kW)
$Ppoi_{t-n}$	Measured power at POI for time $t-n$ (kW)
$Ppoi_{t-n,s-n}$	Forecasted power at POI for time $t-n$ done at period s-n (kW)
$Ppoi_{t,s}$	Forecasted power at POI for time t done at time s (kW)
$Ppoi_{t,t-1}$	Forecasted power at POI for time t done at time $t-1$ (kW)
Q	Battery rated capacity (Ampere-hour)
R	Ideal gas constant (J/mol*K)
SOC_{max}	Maximum SOC (kWh)
SOC_{min}	Minimum SOC (kWh)
SOC_t	SOC for period t (kWh)
$SoHk_t$	State of Health at time t (%)
Ta	Battery internal temperature (K)
$Vami^{AMI}_t$	Inverter voltage measured by AMI at time t (Volt)
$Vmax_{nom}$	Maximum inverter voltage at rated power (Volt)
$Vmin$	Inverter voltage at minimum active power (Volt)
X	Battery market price (€)
X_{red}	Price for reducing active power (€/kWh)
X_t	Electricity retail price at time t (€/kWh)
z	Power-law factor
η_{ch}	Efficient factor for charging
η_{dis}	Efficient factor for discharging
ρ	Ratio of the battery replacement cost (€)
$\sigma(Ibat^{SOCt}_t)$	Severity factor for battery aging in terms of $SOCt$
φ_n	Weight coefficients of ARA

Superscripts

bat	Stationary battery
EMS	Energy Management System
ESS	Energy Storage System
ev	Electric vehicle
$FLEMS$	Flexibility Management System
pv	Photovoltaic Panels
$(')$	Forecasted value

accomplish the flexibility requests of the Distribution System Operator (DSO). Stochastic energy management for microgrids with various types of DERs (power-only, heat-only, fuel cell, combined heat and power units, PV, and wind turbine) and demand response programs is shown by [12]. This close-to-real-time system seeks to decrease operational costs considering price uncertainty, wind speed, solar radiation, and uncontrollable loads. Both [11,12] do not mention the employed DER and flexibility sources, and use an hourly time horizon. [13] has proposed a close-to-real-time EMS to minimize the overall production cost and attend to the DSO flexibility requirements regarding active and reactive power and voltage regulation through real-time measurements and managing combined heat and power units, Energy Storage Systems (ESS), boiler, RES, and thermal and electrical loads every 15-min. Likewise, using 10-min time slots, a real-time optimal schedule controller for residential appliances has been developed by [14] to reduce the end-users energy usage.

The above studies are presented as real-time systems, but their sample, forecasted, or programming time corresponds to 15-min, 30-min, or even hours. To the best of our knowledge, no previous research in the literature has developed a real-time flexibility management system that optimally manages the power dispatch programming in short-term periods (seconds). Therefore, this paper focuses on developing a Flexibility Management System (FLEMS), that optimally manages the energy scheduling generated by an EMS through the real-time power dispatch in short-term periods (seconds), as well as guarantees the generation–consumption balance, quality of electricity supply, profitable operation, and handling the assigned short-term flexibility requests. As additional original contributions, this paper performs a set of sensitivity analyses on relevant parameters of the FLEMS and outlines a coordination scheme between FLEMS and EMS. The remainder of the paper is organized as follows: Section "Control and Management System" exposes the proposed FLEMS and its control and management strategy based on [15]. A reference case study and its results are presented in Section "Reference Case study". A set of sensitivity analyses of relevant variables of the FLEMS and a discussion about the findings are realized in Section "Sensitivity Analysis And Discussion". In the end, conclusions are outlined in Section "Conclusions". Annexes A and B describe the used mathematical formulation of the DERs and their cost models, respectively.

Control and management system

The control and management of power systems with DER could summarize in two complementary schemes. An EMS is in charge of providing an optimal energy program of the DER and long-term flexibility requests, and a FLEMS executes this program in real-time, together with the short-term flexibility requests. This study concentrates on FLEMS and proposes an optimal structure to accomplish its energy objectives, as a low-level controlling actor. Fig. 1 shows the proposed FLEMS structure.

Activation module

Initially, FLEMS possesses an activation module, which determines the initial conditions of the DER, and estimates the reference values from EMS's optimal program based on real-time measurements and control signals transmitted by EMS for the next execution period. The energy exchanges between the grid and end-user at the POI and expected inflexible consumption for the next period are calculated, utilizing the energy balance realized by EMS. The activation module also aims to monitor the power at POI in real-time to detect electricity demands that exceed the maximum consumption and any discharging of energy into the network, since that is not allowed by DSO. The above constraints are also part of the flexibility request for the next period. During the real-time dispatching, this module receives short-term flexibility requirements according to its flexibility potential and Traffic Line Concept (TLC) in line with [16].

Adaptive auto-regression module

The proposed FLEMS uses an Adaptive Auto-regression Algorithm (ARA) to predict the end-user' consumption from the grid, using the historical data, the measured values in real-time, and a set of weight coefficients estimated by training procedure. These stochastic calculations occur with a sample rate over during a rolling horizon base time [17,18]. Eq. (1) defines the ARA's mathematical formulation used in the FLEMS, considering that, each past value initially has the same weight in the prediction process, that is, all weight coefficients will be equal to 1 ($\varphi_n = 1$). These coefficients will be optimized through training procedures with the FLEMS historical data.

$$Ppoi^{,FLEMS}_{t,t-1} = Ppoi^{,EMS}_{t,s} * \frac{1}{min(n,s)} * \sum_{n=1}^{min(n,s)} \varphi_n * \frac{Ppoi_{t-n}}{Ppoi^{,EMS}_{t-n,s-n}} \quad (1)$$

where, $Ppoi^{,FLEMS}_{t,t-1}$ is forecasted power at POI at time t done at time $t-1$ based on n previous time intervals, $Ppoi_{t-n}$ is measured value of power at POI at time $t-n$, $Ppoi^{,EMS}_{t,s}$ is forecasted power at POI for time t done at time s by EMS and $Ppoi^{,EMS}_{t-n,s-n}$ is forecasted power at POI for time $t-n$ done at time s-n by EMS.

Cost–benefit analysis

To make optimal decisions, FLEMS incorporates a Cost–Benefit Analysis (CBA), which is executed to optimize the costs, particularly cost overrun, as well as react to the power deviations at POI. The Eq. (2) represents the CBA, where firstly, the energy cost of the end-user is calculated using the tariff of the Spanish market, PVPC (Precio Voluntario para el Pequeño Consumidor) X_t, forecasted power at POI done by FLEMS, $Ppoi^{,FLEMS}_{t,t-1}$, and forecasted power at POI done by EMS for the same period, $Ppoi^{,EMS}_{t,s}$, as an optimal local baseline for the power system. Secondly, flexibility costs are reckoned as the sum of the costs incurred for the flexibility supply of each DERs, which is defined as the difference between the FLEMS' management cost and reference values from EMS for the same energy program, and execution period. Eq. (3) outlines the mentioned earlier.

$$min \sum_{t=1}^{T} ((Ppoi^{,FLEMS}_{t,t-1} - Ppoi^{,EMS}_{t,s}) * X_t + C^{FLEMS}_{flex}) \quad (2)$$

With,

$$C^{FLEMS}_{flex} = Com^{bat}_t + Cag^{bat}_t + Cur^{pv}_t + Com^{ev}_t + Cag^{ev}_t \quad (3)$$

where C^{FLEMS}_{flex} is the flexibility cost calculated by FLEMS, Cur^{pv}_t is the curtailment cost of PV, Com^{bat}_t, Cag^{bat}_t, Com^{ev}_t, and Cag^{ev}_t are operation and maintenance (O&M), and aging costs of residential and EV battery. In addition, as seen in Eq. (3), only the operation and maintenance costs, as well as the degradation cost of flexible equipment (stationary battery and EV Battery), are taken into account in the objective function of the CBA. These costs are described in Sections "Operation And Maintenance Cost" and "Aging Cost".

Operation and maintenance cost

Optimizing energy resources in power systems begins with defining the costs of each of these and adding the control, monitoring, and communication systems' costs. Diverse authors define multiple cost functions to model the expenses for investment, installation, commissioning, operating, maintenance, and deterioration of the DERs. This study uses a quadratic cost function to model the behavior of the O&M cost. Additionally, this study performances sensitivity analysis on two more employed approaches in the literature (quadratic and linear functions) to show the influence of the cost formulations on the final results of the FLEMS. More details about the selected cost functions and the involved technical and economic aspects related with the cost are mentioned in Annex B.

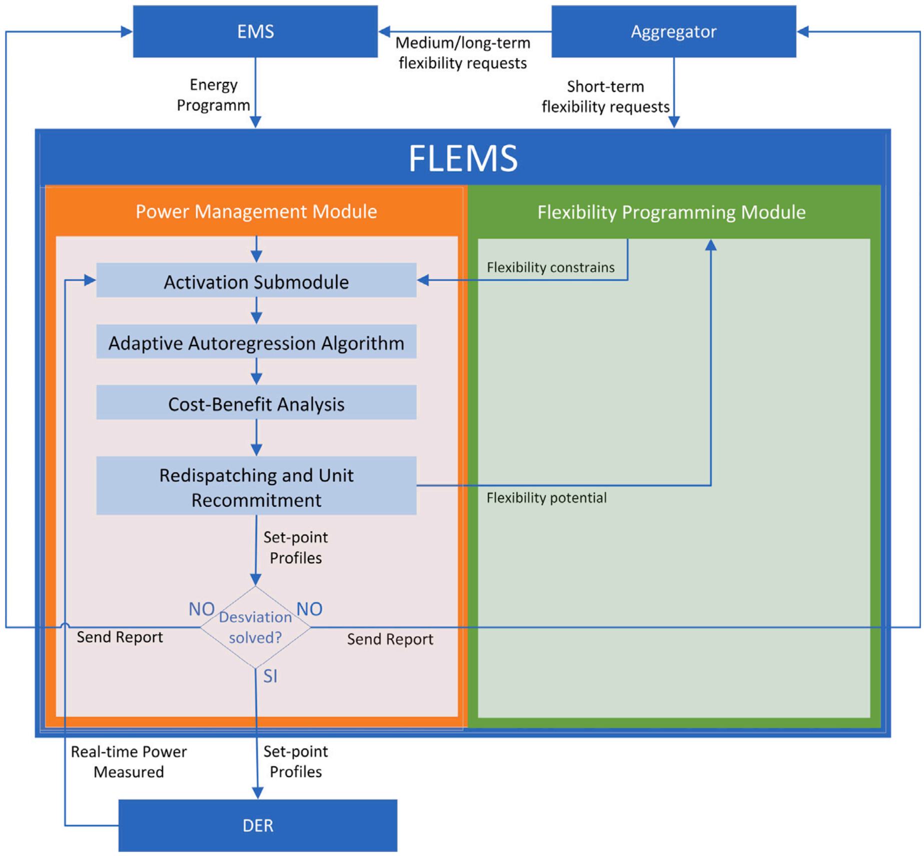

Fig. 1. Flexibility management in power systems with distributed energy resources.

Aging cost

Along with the O&M cost, the aging cost of the ESS must be adequately estimated to optimize its operation to minimize energy costs and provide flexibility services. [19,20] describes mathematical models based on reducing battery life according to a severity factor. [21] proposes a model that quantifies the impacts on the useful life concerning the charge and discharge cycles spent with respect to the total number of cycles allowed. Another model used for flexibility service optimization problems is based on the loss of the State of Health ($SoHk_t$) of the battery done by [19]. This model calculates the negative effect of over-cycling through loss of battery capacity in terms of 1 C-rate, activation energy, and internal battery temperature. The Annex B mentions three Aging Cost Models (ACM) mentioned previously and their mathematical formulations. These aging cost models are tested in Section "Aging Cost Functions".

Redispatching and unit recommitment modules

Redispatching (RDM) and Unit Recommitment Modules (URM) aim to respond to critical conditions, which could force DER set-point profiles to the CBA to solve voltage violations, reactive power dispatching, planned and unplanned islanding, reconnection, black start, short-term flexibility requests, among others. Due to the above scenarios and during real-time dispatching, both ARA and CBA optimization modules must update with these new conditions. This study will only include the management of short-term flexibility requests regarding the maximum and minimum power exchanges at POI.

Essentially, RDM and URM apply the same objective function explained in Section "Cost–Benefit Analysis" for CBA, which minimizes the energy cost and cost overruns in real-time dispatching, taking into account that some DER's power set-point profiles are fixed and forced in CBA, as well as the constraints are updated in order to supply flexibility. A restricted nonlinear multivariate function library from Matlab solves the refreshed CBA.

Reference case study

To prove the effectiveness of the proposed management system (FLEMS), a single-family household is selected as a case study. The real-time consumption, PV generation, and EV charging sessions are collected from DataPort Inc. Street 2022 for residential prosumers [22]. The prosumer has a 6.6 kW PV, a 10 kWh residential battery, and a 10.4 kW EV charging station for household facilities (Chevrolet Volt). This study defines a contracted power of 2.6 kW and is not allowed any sell-back electricity to the grid. The CBA applies the Spanish dynamic electricity tariff (Precio Voluntario Pequeño Consumidor, PVPC) as in [4] and its power term value and taxes are neglected.

To execute the FLEMS, firstly, EMS must provide the energy program for DERs for the next 24 h divided into 15-min periods. In this case, the Pyomo optimization library generated the corresponding energy program for January 14th of 2018. FLEMS's activation module receives the energy program and initializes its reference values (P_t^{pv} = 600 W, $Ppoi_{t,s}^{,EMS}$ = 350 W, $Pinf_t^{,EMS}$ = 900 W, $P_t^{,bat}$ = 0 W, $P_t^{,ev}$ = 0 W, Penalty for exceeding contracted power = 1.4064 €/kWh, $Pl_t^{bat} = Pl_t^{ev} = Pl_t^{pv}$ = 158.5 W, X_t = 0.04 €/kWh, P_{nom} = 2600 W, P_{min} = 0 W), considering linear power dispatching of the DER every 15 min and ACM1.

FLEMS focuses on the 15 min beginning January 14th at 17:00, sampling that period into 15 s sub-periods according to the ARA's sample time, three measured past values, and weight coefficients equal to 1 ($\varphi_n = 1$). Regarding the cost models, the quadratic cost function and ACM1 are selected as reference cases. Therefore, the a_c and c are defined previously as 2 €/kW^2 and 1 € respectively in line with [23]. The simulation was carried out using the Matlab optimization library with a laptop EliteDesk with Intel Core i7 at 2.60 GHz and 8 GB of RAM Memory. The following three events were scheduled:

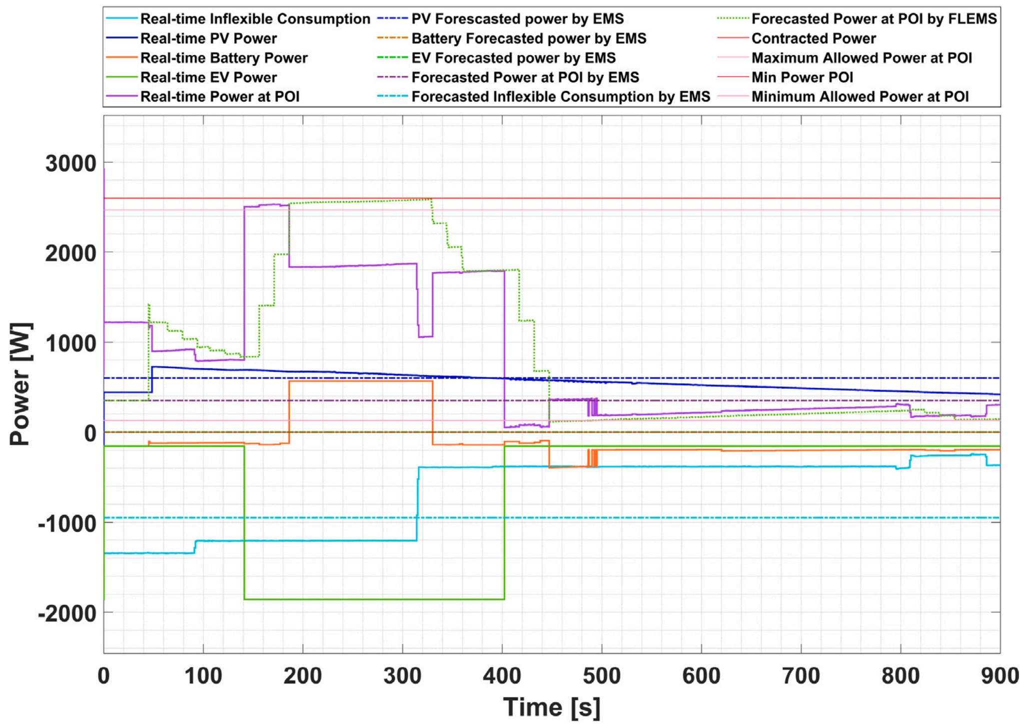

Fig. 2. Real-time energy program execution under FLEMS from 17:00 to 17:15 of January 14th.

- Excess PV Curtailment: FLEMS estimates a solar curtailment tolerable of 0.004 kWh due to a forecasting error about PV production. When this limit is surpassed, FLEMS reformulates a new PV set-point profile.
- Unexpected EV Charging session: A unexpected EV charging session is scheduled from 141st to 402th seconds. FLEMS optimizes the cost overrun, preventing exceeding the redefined maximum power at POI (2600 W)
- Undesired active power exchange with the network: Possible energy injections to the grid could be done from 402nd second to the end of the simulation period according to the variation of the inflexible consumption and real-time PV production.

Fig. 2 shows real-time values (continuous lines) and forecasted values from EMS (dashed lines) for inflexible consumption (light blue), PV production (dark blue), power supplied from the grid at POI (lilac), power discharging and charging of the battery (orange) and EV battery (green), as well as power limits, contracted and fed into the grid (red), and tolerance range (5%) (pink). Besides, the dotted green line represents the forecasted power from FLEMS at POI.

During the real-time dispatching, FLEMS detected solar curtailment because of a forecasting error from EMS. FLEMS adjusts solar production according to the real-time AMI-voltage-based method explained in [15]. That happens at the 48th second. Lately, FLEMS manages the power of DER optimally in front of an unexpected EV charging session, which would increase the energy supplied from the grid at POI to the maximum permissible value. As a result of CBA, FLEMS acts on energy transfer to the battery at the 186th second, minimizing the end-user's consumption until the 330th second when this situation finishes due to the decrease in inflexible demand. Finally, FLEMS charges the battery to avoid any sell-back electricity to the grid in 447th, 486th, 620th, and 824th seconds according to the available power of DERs, and the application of ARA, CBA, and redispatching and unit recommitment modules.

Following the EMS set-point power of DERs, the total energy cost achieves 0.62 € during the observed time, since the charging of the electric vehicle is prevented and thus, the application of the corresponding penalty (5 €/kWh). Allowing the unexpected connection of the EV reduces the total cost to 0.2 €, considering that the penalty for exceeding the contracted power is applied (1.4064 €/kWh). The incorporation of FLEMS and its management of cost overruns and unexpected events reduces costs to 0.11 €, an estimated saving of 45%

Sensitivity analysis and discussion

This study proposes a set of sensitivity analyses about critical parameters of the proposed flexibility management system. Firstly, the ARA is analyzed considering different sample periods and past series values in the objective function of the case study. Later, two cost formulations are involved in the reference case study to identify their influence on the expected savings of the proposed management system. Lastly, three penalty levels are regarded in the objective function of the case study to evaluate their impact on energy cost savings. As evaluation parameters, the calculation time, the total energy cost and savings, the number of micro and macro-cycles of the storage elements, and the depth of the loading and unloading cycles are established.

Impact of ARA parameters

As indicated in Section "Adaptive Auto-regression Module", the FLEMS uses an ARA for forecasting the power at POI according to their past series values, the forecasts made by EMS, and weight coefficients. As mentioned previously, these coefficients are fixed ($\varphi_n = 1$), therefore, the sample period and the past series values are analyzed in this section to define their impact on the effectiveness of the FLEMS. Here, the following sensitivity analyses are based on the reference case study, that is, the total energy cost of 0.2 €, quadratic formulation for O&M costs as indicated in Section "Operation And Maintenance Cost", ACM1, and penalty for exceeding the contracted power of 1.4064 €/kWh.

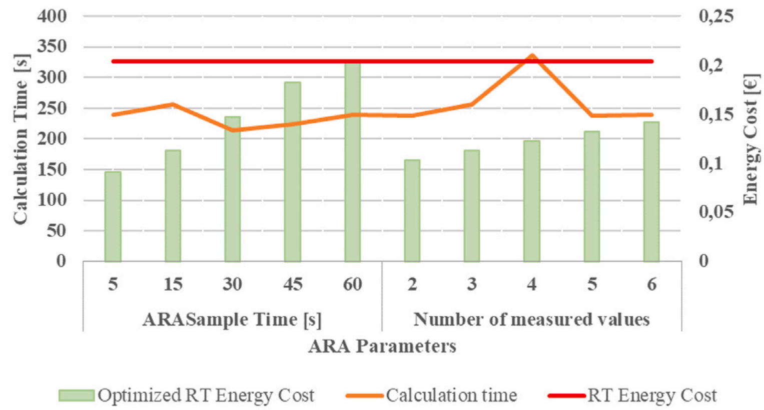

Fig. 3. Impact ARA sample time and number of measured values on calculation time and total energy cost.

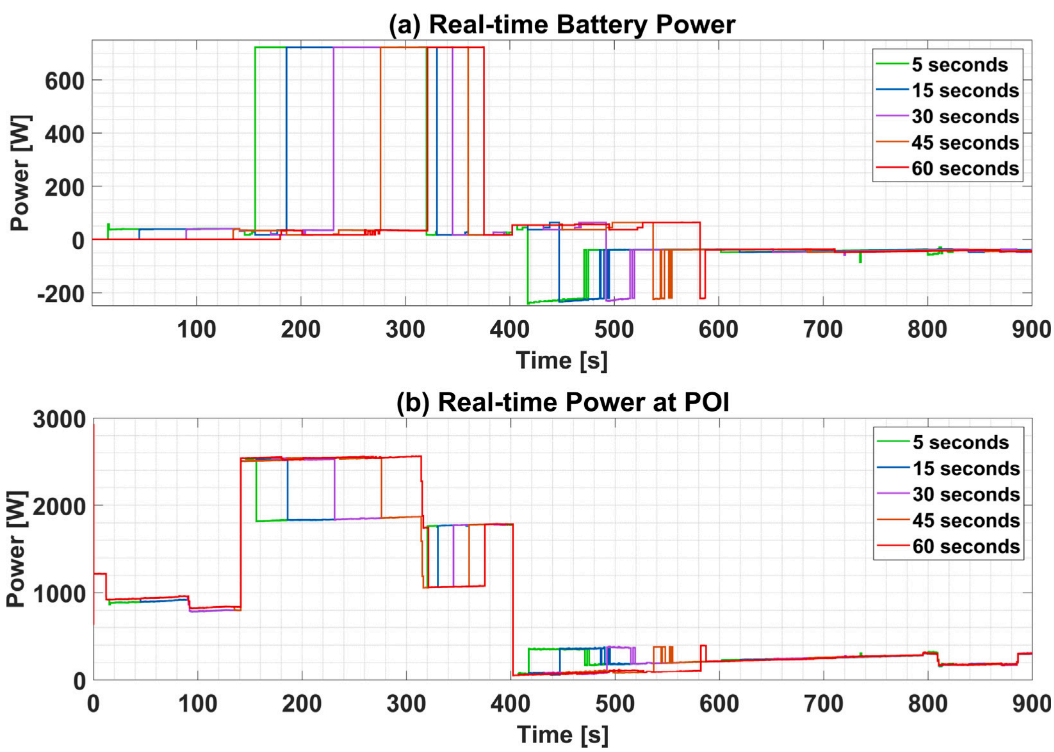

Fig. 4. Impact of ARA sample time on: (a) Real-time battery power, (b) Real-time power at POI.

ARA sample time

A sample period must be appropriately selected to perceive the changes that occur in the variable to be controlled and reduce excessive forecasting deviations during real-time execution. The ARA' sample time determines the frequency at which CBA must be evaluated, updating the set profiles of DERs. Therefore, special attention should be paid to this period. For sensitivity analysis, the reference case study has been modified with five forecasting periods, from 5 to 60 s. The results are summarized in Figs. 3 and 4, considering calculation time, total energy cost, and the number of partial cycles of the batteries.

As seen in Figs. 3 and 4, large sampling periods ($n > 30$ s) react late to power deviations in the observed period, increasing the cost overruns until equalizing to the costs without FLEMS ($n = 60$ s). Therefore, going deeper into the calculation methodology of this period could guarantee the expected savings. In addition, short sampling periods ($n < 30$ s) produce more significant savings but represent longer computational calculation times (in average 236 s during 900 s of execution), reducing the available time for the communication of the instructions, processing time, or solving failures in the sensors (noise or time delay) taking into account that 13 s are required for measuring, computing and communicating the control set-point profiles according to [18].

Here, this sampling period can be fixed for whole sub-periods (every 15 min) or vary in time according to the volatility of the power dispatch or the characteristics of the power system, if the end-user belongs to residential, industrial, and commercial sectors, as well as if they are energy communities or aggregators. This question should be studied in future works.

Past series values

Together with the sampling frequency, the past series values form the heart of the ARA forecasting technique, given that, as mentioned previously, the weight coefficients are initialized ($\varphi_n = 1$) and will be optimized according to the produced effectiveness historical data of the FLEMS. For reference case study, a third grade ($n = 3$) was estimated for a residential prosumer according to [17,18]. The prediction accuracy and variability of the forecasted values are modified accordingly to

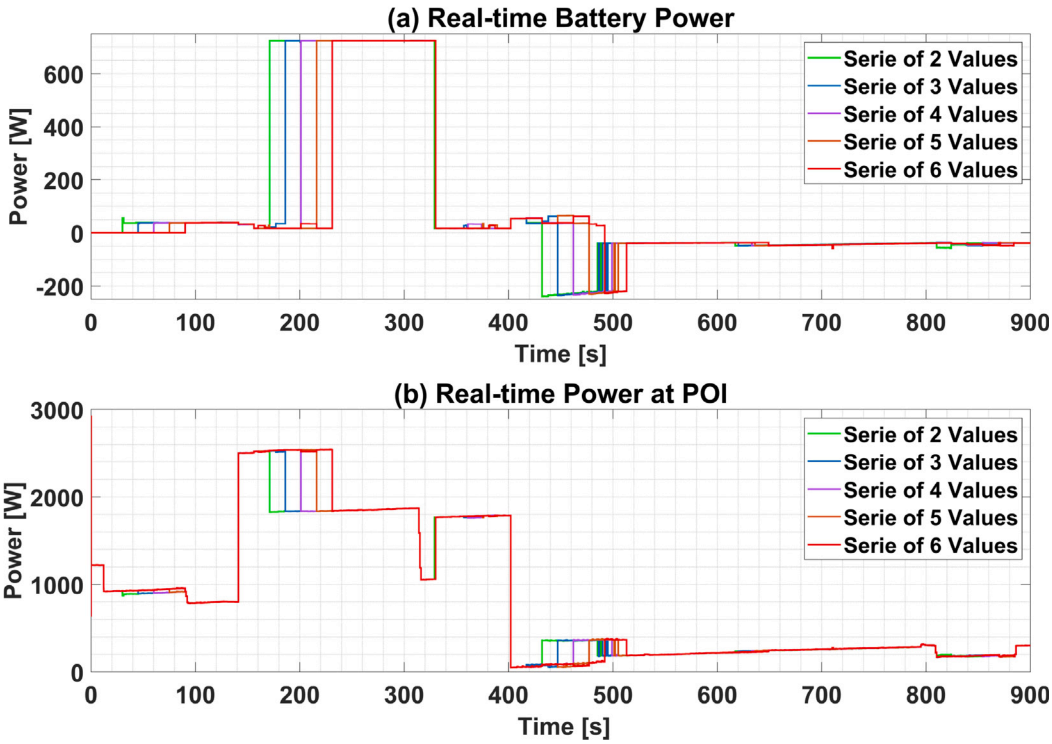

Fig. 5. Impact of number of measured values of ARA on: (a) Real-time battery power, (b) Real-time power at POI.

past series values. Furthermore, this study varies the number of values passed from 2 to 6 in the reference case study to show its effects in reducing cost overruns in real-time and the DERs' behavior.

As seen in Figs. 3 and 5, implementing four or more measured past values is more resilient against irrelevant variations in the control parameters in 357th, 617th, 710th, and 810th seconds, allowing for damping these changes without activating FLEMS unnecessarily, in other words, without over cycling the battery (less aging cost). The relevant changes are usually perceived with a delay that implies a reduction in the savings. Also, using more measured past values implicate more calculation time (in average 270.8 s during 900 s of execution). A series composed of two or three measured values allow more significant savings due to the rapid reaction to changes, and the excessive uses of the ESS are not substantial. A long-term economic analysis and the type of ACM could modify this premise.

Impact of cost models

As analyzed in the reference case, controlling the cost overruns and supplying flexibility services are linked with the cost models applied in CBA. Two sensitivity analyses of the cost formulation exposed in Sections "Operation And Maintenance Cost" and "Aging Cost" are performed in this Section.

Operation and maintenance cost functions

As referred in Section "Cost–Benefit Analysis", two mathematical formulations for modeling the O&M cost of the ESS are included in the reference case study. Considering the Eqs. (B.1) and (B.2), the linear modeling is completed with the life-cycle cost coefficient (C_{lcc}), which was estimated in 0.80 €/kWh by [24] for lithium-ion batteries for frequency regulation and increase of self-consumption applications. 34 small cycles per day at 5% of DoD are stipulated. On the quadratic modeling side, the formulation is completed with the parameters mentioned in the reference case study.

Fig. 6 shows the impact of the diverse mathematical formulations of the O&M cost on battery operation and power at POI. With the other parameters unchanged, quadratic and linear modelings are incorporated in the reference case study. The quadratic modeling estimates the usage of the storage equipment as more expensive than the linear model in real-time. Therefore, lower rates of battery use, albeit with more significant savings (45%) than the lineal approach (27.81%). On the other hand, the savings are significantly diminished if the lineal O&M cost model is applied in CBA. Finally, the system exchange energy to the grid at 320th second when the lineal modeling is utilized for the O&M costs, which increases the cost overruns.

Aging cost functions

To embody the sensitivity of the aging cost of the ESS adopted in this proposed control and management system, three cases are considered to evaluate each ACM, as illustrated in Section "Aging Cost". These three cases are based on the reference case study but a diverse ACM is applied in each case. As the main finding, aging cost models demonstrated low influence in real-time control of the DERS. This influence grows over time, depending on its mathematical definition. Models based on micro and macro cycles quantify more degradation values than models related to C-rate, internal temperature, battery activation energy, or severity factors. Conversely, the ACM has a large impact in the estimation of the total savings. For instance, Fig. 7 shows the total energy costs after the FLEMS application for the lineal and quadratic formulations of O&M costs, and each ACM. As can be seen, ACM1 based on the severity factor, estimates a lower deterioration cost than the rest of the models. ACM2 records the maximum value of aging cost, even achieving the same value of the total energy cost without FLEMS for the lineal O&M cost model, due to the number of micro-cycles (7) spent out of the total cycles of the battery's useful life. The savings with respect to the reference case base are 26.2% and 35% for ACM2 and ACM3, respectively. These results show that the total savings vary from 45% to 26.2% depending on the selected ACM.

Impact of penalty for exceeding contracted power

Penalties for exceeding the contracted power or injecting electricity into the grid are critical parameters in CBA that modify the operation

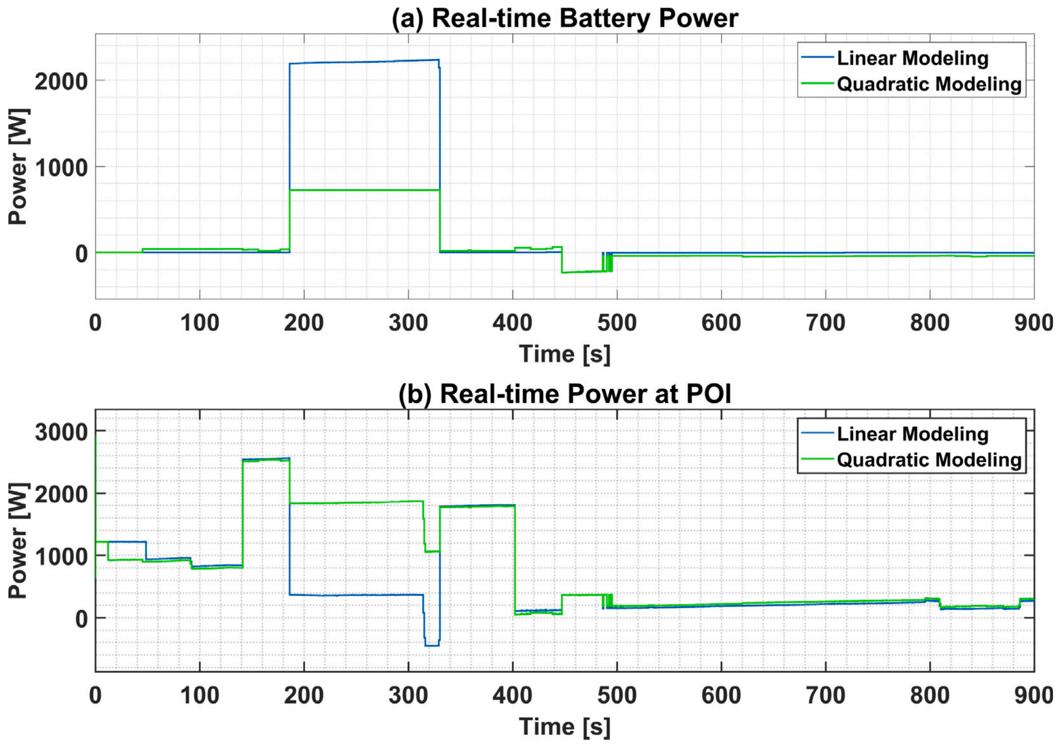

Fig. 6. Impact of O&M cost models on: (a) Real-time battery power, (b) Real-time power at POI.

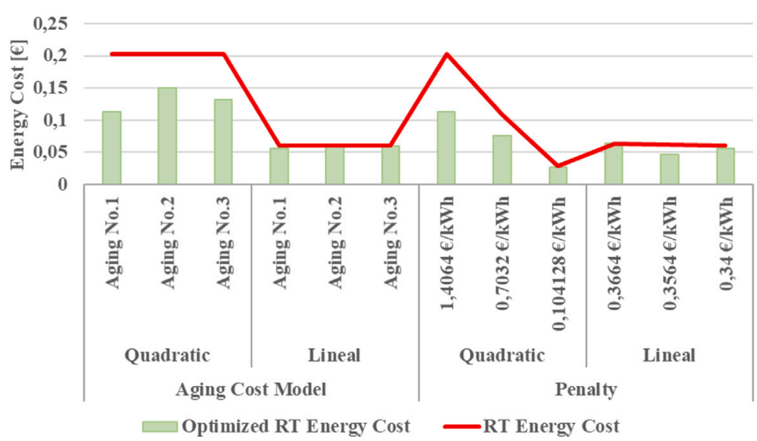

Fig. 7. Impact of aging cost models and penalties on total energy cost according to O&M cost model.

of the power system in real-time. In Spanish, residential users with contracted power below 15 kW do not have penalties associated with excess power. To estimate the costs, two tariffs, 1.4064 €/kWh and 0.104128 €/kWh have been taken from two energy resellers for residential users with power greater than 15 kW or less than 15 kW with uninterruptible equipment. Additionally, intermediate rates are used to show the behavior of the cost models used in this study (linear and quadratic). These intermediate rates are proportional to the rates defined by the energy traders.

First of all, Fig. 7 shows the total energy cost estimated by the linear and quadratic models according to the operation of FLEMS (green bars) versus the total energy cost without FLEMS of the power dispatch in real-time (red lines), highlighting the used intermediate rates of penalty. As mentioned in Section "Operation and Maintenance Cost Functions", the savings are significantly diminished if the lineal O&M cost model is applied in CBA. Therefore, for lineal modeling of O&M cost, only penalties between 0.34–0.3664 €/kWh have an impact on the real-time operation of the system, since the FLEMS is not activated (<0.34 €/kWh) or acts until achieving the same energy cost without FLEMS (>0.3664 €/kWh). The savings for penalties of 0.34 €/kWh and 0.3564 €/kWh were 25.5% and 6.44%, respectively. Regards to quadratic modeling, minor penalties reduce the potential savings of the FLEMS, from 45% to 30% (0.7032 €/kWh) and 6.55% (0.104128 €/kWh).

According to the above, linear modeling is more sensitive to the variation of penalties than quadratic models, which must be adjusted to a short range of convenient values to avoid the charge and discharge depth of the battery and possible energy sell-back to the grid, for instance between 315th and 320th seconds for a penalty of 0.3664/kWh, as seen in Fig. 8. Otherwise, the available range for the quadratic model is large, where high prizes represent high potential savings. Lastly, other approaches define this penalty as the costs of a power outage of the grid or the flexibility service's prices. This approach must be taken into account in future research.

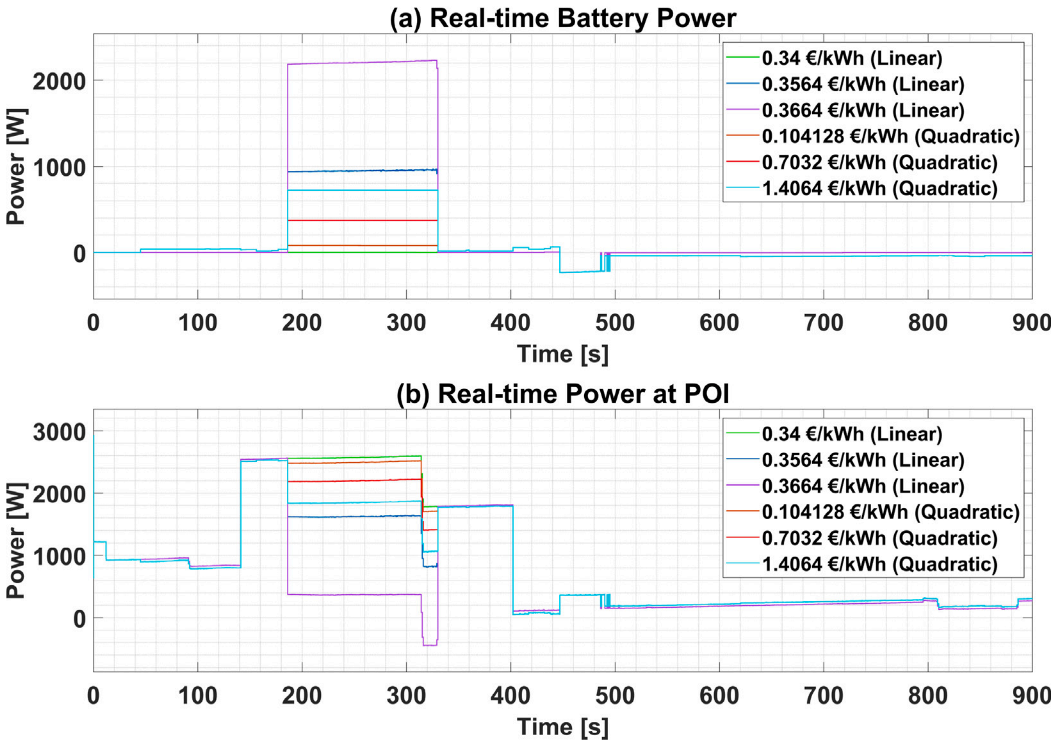

Fig. 8. Impact of penalties and O&M cost function on: (a) Real-time battery power, (b) Real-time power at POI.

Conclusions

A flexibility management system was used to minimize the energy cost of an end-user installation that contains the following DER: PV panels, residential battery, EV charging station, and controllable loads. The proposed system comprises a forecasting module based on an adaptive auto-regression algorithm, a CBA, power redispatching, and unit recommitment modules. The main conclusions are as follows:

- Initially, a single-family household was chosen to execute FLEMS as a reference case study. The results indicates 45% of savings in the total energy cost of the system if the ARA parameters mentioned in Section "Reference Case study", quadratic modeling of the O&M cost, severity factor for measuring the degradation cost of ESS and specific penalty are applied. Several sensitivity analyses on ARA parameters, mathematical formulations for O&M and aging costs, and penalties for surpassing the contracted power were carried out without improving the results obtained in the reference case study.
- The sensitivity analysis results show that the sample time must be 30 s to obtain relevant savings without high computational costs. Smaller sample periods provide more savings and higher operating expenses but collide with the required time to communicate, process and receive the power set-point profiles. Values over 60 s do not produce benefits. On the other hand, two or three measured past values are enough to predict power at POI adequately. Although the calculation time remains constant for various past measured values, the savings obtained decrease due to the attenuation of power changes in the POI.
- From reference case study results with different mathematical formulations for O&M cost, quadratic modeling quantifies higher operation and maintenance costs and, therefore, lower rates of battery use, albeit with more significant savings (45%) than lineal approach (27.81%). In addition, the quadratic formulation is less sensitive to irrelevant changes, reducing the number of micro-cycles of the battery and its depth of charge and discharge. Lastly, linear modeling has proven to be more volatile to the penalty for exceeding contracted power than quadratic one. Therefore, only a small and specific range of penalty values can guarantee the correct operation of the control system, unlike quadratic modeling, which allows higher degrees of freedom of choice.
- The ACM did not directly influence the control of DERs in real-time. This influence grows over time, depending on its mathematical definition. Models that account for micro and macro cycles show higher values than models based on C-rate, internal temperature, battery activation energy, or severity factors. Quadratic formulation costs accelerate the relevance of the aging cost into CBA.
- As seen in Fig. 8, the penalty for exceeding contracted power considerably impacts the formulation of the CBA and the results of management systems in real-time. Linear cost models have a more remarkable sensitivity to the variation of penalties than quadratic models, given that the range of values that active the FLEMS are limited, from 0.34€/kWh to 0.3664€/kWh, and savings are reduced strongly (from 45% to 6.44%).

As future work, a sensitivity analysis of the constants used in the ARA model based on historical housing data should be carried out to confirm the assumption that the values found in [17,18] for residential users. To ensure the integrity and dependability of the FLEMS, it is also necessary to conduct a failure analysis of the communications system, sensors, or processing. On the other hand, the training procedure of the weight coefficients of ARA must be performed to improve the predictions and algorithm performance, according to historical data of FLEMS execution. Finally, experimental validation is necessary for residential, commercial, and industrial users to adopt FLEMS for commissioning.

Declaration of competing interest

The authors declare the following financial interests/personal relationships which may be considered as potential competing interests: Jose-Fernando Forero-Quintero reports financial support was provided by Spain Ministry of Science and Innovation.

Data availability

Data will be made available on request.

Acknowledgment

This work has been supported by the FLEXRED project under Grant PRE2019-090100 funded by MCIN/AEI/10.13039/501100011033 and by "ESF Investing in your future". The research of Jose-Fernando Forero-Quintero has received support under Grant RTI2018-099540-A-I00 funded by MCIN/AEI/10.13039/501100011033 by "ERDF A way of making Europe".

Ethical statement

• This material has not been published in whole or in part elsewhere.
• The manuscript is not currently being considered for publication in another journal.
• All authors have been personally and actively involved in substantive work leading to the manuscript and will hold themselves jointly and individually responsible for its content.

Appendix A. Mathematical models

This appendix presents the mathematical models of distributed energy resources and their operational constraints.

Stationary battery

As an Energy Storage System (ESS), the residential battery's mathematical model begins with the State of Charge (SOC) equation. The SOC depends directly on the efficiency factor for charging and discharging, as well as minimum SOC_{min}^{bat} and maximum SOC_{max}^{bat} levels of charge, in order to preserve the battery life. The Eqs. (A.1) and (A.2) define the SOC's behavior of the battery. As part of the model, the power ramp rates are also considered for a certain period *t*, both for charging and discharging. The Eqs. (A.3) and (A.4) outline these rates.

$$SOC_t^{bat} = SOC_{t-1}^{bat} + Ech_t^{bat} * \eta_{ch}^{bat} - \frac{Edis_t^{bat}}{\eta_{dis}^{bat}} \tag{A.1}$$

$$SOC_{min}^{bat} \leq SOC_t^{bat} \leq SOC_{max}^{bat} \tag{A.2}$$

$$Ech_t^{bat} \leq \frac{Pch_{max}^{bat}}{N^{bat}} \tag{A.3}$$

$$Edis_t^{bat} \leq \frac{Pdis_{max}^{bat}}{N^{bat}} \tag{A.4}$$

where Pch_{max}^{bat} and $Pdis_{max}^{bat}$ are the maximum power for charging and discharging for the period N^{bat} given by the battery's manufacturer, respectively.

Electric vehicle

As mentioned in the residential battery section, the SOC in an EV battery is delineated in Eqs. (A.5) and (A.6). The Eqs. (A.7) and (A.8) limit the energy charged Ech_t^{ev} or discharged $Edis_t^{ev}$ by EV battery for the recommended period N^{ev} according to maximum power for charging Pch_{max}^{ev} and discharging $Pdis_{max}^{ev}$.

$$SOC_t^{ev} = SOC_{t-1}^{ev} + Ech_t^{ev} * \eta_{ch}^{ev} - \frac{Edis_t^{ev}}{\eta_{dis}^{ev}} \tag{A.5}$$

$$SOC_{min}^{ev} \leq SOC_t^{ev} \leq SOC_{max}^{ev} \tag{A.6}$$

$$Ech_t^{ev} \leq \frac{Pch_{max}^{ev}}{N^{ev}} \tag{A.7}$$

$$Edis_t^{ev} \leq \frac{Pdis_{max}^{ev}}{N^{ev}} \tag{A.8}$$

The above-mentioned constraints are incorporated in the CBA and objective function.

Photovoltaic panels

There are equivalent schemes to represent photovoltaic panels as a distributed generation. Inflexible and controllable generation are the most common proposals. In this study, a curtailable reducible model is used. The amount of energy produced by curtailable reducible photovoltaic panels, P_t^{PV}, is described in Eq. (A.9) in terms of predicted PV production at instant t $P_t^{\prime PV}$.

$$0 \leq P_t^{PV} \leq P_t^{\prime PV} \tag{A.9}$$

In addition, PV production is reduced to a certain energy volume or even interrupted to generate flexibility or management deviations. In turn, the cost for reducing this generation $Cred_t^{PV}$ due to forecasting errors are stated in Eq. (A.10), and Eqs. (A.11) and (A.12) respectively, where X_{red}^{PV} is the price for reducing PV production.

$$Cred_t^{PV} = \sum_{t=1}^{T} X_{red}^{PV} * (P_t^{\prime PV} - P_t^{PV}) \tag{A.10}$$

$$Cur_t^{PV} \leq Cur_{tol}^{PV} \tag{A.11}$$

$$Cur_t^{PV} = \sum_{t=1}^{T} \frac{Vami_t - Vmax_{nom}}{Vmin - Vmax_{nom}} * (P_{nom}^{PV} - P_{min}^{PV}) \tag{A.12}$$

where Cur_{tol}^{PV} is the tolerable level of solar curtailment, $Vami_t$ is the voltage recorded by Advanced Metering Infrastructure (AMI), $Vmax_{nom}$ is the maximum voltage at which PV system generates its rated power P_{nom}^{PV}. $Vmin$ is the voltage at which the system produces its minimum active power P_{min}^{PV}

Power balance

Generated and consumed power must be equal during the real-time energy planning execution, considering the ESS's losses related to cables and charging and discharging efficiencies. The power balance constraint is given by Eqs. (A.13) and (A.14).

$$Ppoi_t = Pinf_t + Pl_t - P_t^{bat} - P_t^{ev} - P_t^{pv} \tag{A.13}$$

$$Pl_t = Pl_t^{bat} + Pl_t^{ev} + Pl_t^{pv} \tag{A.14}$$

where $Ppoi_t$ is the power at POI at time *t*, which can only be positive as DSO restricts prosumers' energy injection into the grid. P_t^{ev}, and P_t^{bat} are the power discharged (+)/charged (-) of the EV battery and residential battery, respectively. Also, the power losses of the system must be included.

Appendix B. Cost models

This appendix describes the cost models used in this study, related to the O&M and aging cost. Expenses of the control, monitoring, and communication systems are overlooked, due to the paper seeks to test important parameters of the control and management strategy of the FLEMS. The full costs can be reviewed in [25].

Operation and maintenance cost

The operation and maintenance (O&M) cost encompasses diverse aspects of the assets, expected degradation during life-time, ordinary maintenance sessions, control and management cost, among others, depending on the cost analysis approach. For this study, linear and quadratic functions are selected to model the (O&M) cost, including some aspects that are explained as follows:

- Linear Cost Modeling: Authors as [26,27] express the total cost of DERS using a linear cost model composted of the DER' operation power P_t^{ESS} and a coefficient based on life-cycle cost assessment of the DER. Such coefficient involves power conversion system cost, balance-of-plant cost, O&M cost, and the type of application and battery technology. Even, [27,28] raise a piece-wise linear approximation model for the power-only unit's cost function modifying the life-cycle cost coefficient over time or according to load shedding of the power system. Likewise, [21] defines the cost of the environmental externalities (CO2, SO2, NOx) as assumed to be a linear function of the output power of DER. Remember that this linear model is simplified as shown in Eq. (B.1), correctly selecting the life-cycle cost coefficient for real-time applications.

$$Com_t^{ESS} = C_{lcc} * P_t^{ESS} \tag{B.1}$$

- Quadratic Cost Modeling: The quadratic cost modeling includes the considerations incorporated in the linear perspective, appending terms to represent the energy supply and management cost of the active power of DERs. For instance, [23,29] describe a generation cost for conventional generators as a quadratic function in terms of active power. [30], and [31,32] define that the operation costs of distributed generators, batteries, wind turbines, and PV could model by quadratic functions. For [33], the quadratic term is related to the production and supply cost of renewable DGs and ESS, the linear term corresponds to the participation of the power system in the energy market according to the possible real-time electricity prices, and the last term corresponds to the fixed cost for the microgrid's operation and maintenance. As mentioned [21,30], only the terms a_c and c are taken into account in the real-time context. The above is expressed in Eq. (B.2):

$$Com_t^{ESS} = a_c * (P_t^{ESS})^2 + c \tag{B.2}$$

Aging cost

Numerous studies highlight the relevance of aging cost on battery operation programming in electric systems with DERs. The drop in the state of health of batteries has diverse causes, including excessive charge–discharge cycles, over-temperature, excessive deviations of the optimal SoC, non-optimal depth of discharge (DoD), over-charge, and over-discharge, among others. According to each factor, various mathematical models define the subsequent degradation. This appendix describes three main formulations for real-time analysis.

- Aging cost model 1 (ACM1): As mentioned in the case study, the aging model is based on the severity factor, which quantifies the effects of a given cycle concerning the nominal cycle supplied by the manufacturer to achieve the battery life cycle. According with [19,20], the aging model for lithium-ion battery is as follows:

$$Cag_t^{ESS} = X^{ESS} * \frac{Ah_t^{ESS}}{Q^{ESS} * Clife^{ESS}} \tag{B.3}$$

$$Ah_t^{ESS} = \frac{1}{T} * \int_0^T \sigma(IK_{t,SOCt}^{ESS}) * Ik_t^{ESS}\, dt \tag{B.4}$$

$$\sigma(Ik_{t,SOCt}^{ESS}) = \frac{\int_0^T Ik_t^{ESS}\, dt}{\int_0^T Inom^{ESS}\, dt} \tag{B.5}$$

where, Q^{ESS} is battery rated capacity in Ah, X^{ESS} is battery market price, Ah_t^{ESS} is the total aging effect caused by cycling, $Ik_{t,SOCt}^{ESS}$ is measured current at given *SOCt* and $Clife_t^{ESS}$ is battery life cycle at time *t*.

- Aging cost model 2 (ACM2): Unlike the previous model, the capacity loss of the battery is related to the number of considered micro- and macro-cycles (events), *N*, and an aging factor in terms of the average SOC of each cycle, $Kag_{t,SOC}^{ESS}$, as well as the maximum of the possible cycles in a battery lifetime to the given DoD level, $Npos_{t,DOD}^{ESS}$. Taking into account to [21], the aging cost in total observation time is calculated as:

$$Cag_t^{ESS} = 0.5 * Q^{ESS} * X^{ESS} * \sum_{t=1}^{N} \frac{Kag_t^{SOC}}{Npos_t^{DOD}} \tag{B.6}$$

where the Stress number (SN) and SoC aging factor curves of a lithium-ion battery are used to determine the Kag_t^{SOC} for Eq. (B.6).

- Aging cost model 3 (ACM3): [19] suggests the battery's C-rate, activation energy ($Ea(c)$), and internal temperature (Ta) significantly impact the number of allowed charge–discharge cycles before End-Of-Life (EOL) as the battery performance and its State of Health ($SoHk_t$). Therefore, Eqs. (B.7), (B.8), and (B.9) are employed to formulate the total aging cost.

$$Cag_t^{ESS} = \rho * \Delta SoHk_t \tag{B.7}$$

$$\Delta SoHk_t = -\frac{Ik_t}{2 * Nk(c, Ta) * Cn_t} \tag{B.8}$$

$$Cn_t = B(c) * e^{-\frac{Ea(c)}{R*Ta}} * Ah(c)^z \tag{B.9}$$

where the C-rate curve describes the relation of a specific discharge rate of the battery with its maximum capacity. A 1 C rate means the entire battery can be discharged in one hour. $Nk(c, Ta)$ is the number of cycles before EOL in terms of *c* and *Ta* and Cn_t is the capacity loss at time *t*.

References

[1] Coban HH, Lewicki W. Flexibility in power systems of integrating variable renewable energy sources. J Adv Res Natural Appl Sci 2023;9(1):190–204. http://dx.doi.org/10.28979/jarnas.1137363.

[2] Cacioppo M, Favuzza S, Ippolito MG, Musca R, Riva Sanseverino E, Telaretti E, Zizzo G, Arnone D, Mammina M. Demand project: An algorithm for the assessment of the prosumers' flexibility. In: 2020 IEEE 20th Mediterranean electrotechnical conference. MELECON, 2020, p. 565–9. http://dx.doi.org/10.1109/MELECON48756.2020.9140612.

[3] Bremdal BA, Sæle H, Mathisen G, Degefa MZ. Flexibility offered to the distribution grid from households with a photovoltaic panel on their roof: Results and experiences from several pilots in a Norwegian research project. In: 2018 IEEE international energy conference. ENERGYCON, 2018, p. 1–6. http://dx.doi.org/10.1109/ENERGYCON.2018.8398848.

[4] Barja-Martinez S, Rucker F, Aragues-Peñalba M, Villafafila-Robles R, Munne-Collado, Lloret-Gallego P. A novel hybrid home energy management system considering electricity cost and greenhouse gas emissions minimization. IEEE Trans Ind Appl 2021;57(3):2782–90. http://dx.doi.org/10.1109/TIA.2021.3057014.

[5] Elma O, Selamogullari US. A new home energy management algorithm with voltage control in a smart home environment. Energy 2015;91:720–31. http://dx.doi.org/10.1016/j.energy.2015.08.094, URL https://www.sciencedirect.com/science/article/pii/S0360544215011706.

[6] Pipattanasomporn M, Kuzlu M, Rahman S. An algorithm for intelligent home energy management and demand response analysis. IEEE Trans Smart Grid 2012;3(4):2166–73. http://dx.doi.org/10.1109/TSG.2012.2201182.

[7] Shakeri M, Shayestegan M, Abunima H, Reza SS, Akhtaruzzaman M, Alamoud A, Sopian K, Amin N. An intelligent system architecture in home energy management systems (hems) for efficient demand response in smart grid. Energy Build 2017;138:154–64. http://dx.doi.org/10.1016/j.enbuild.2016.12.026, URL https://www.sciencedirect.com/science/article/pii/S0378778816318369.

[8] Vieira Pombo A, Murta-Pina J, Fernao Pires V. Multiobjective formulation of the integration of storage systems within distribution networks for improving reliability. Electr Power Syst Res 2017;148:87–96. http://dx.doi.org/10.1016/j.epsr.2017.03.012, URL https://www.sciencedirect.com/science/article/pii/S0378779617301128.

[9] de Oliveira e Silva G, Hendrick P. Photovoltaic self-sufficiency of belgian households using lithium-ion batteries, and its impact on the grid. Appl Energy 2017;195:786–99. http://dx.doi.org/10.1016/j.apenergy.2017.03.112, URL https://www.sciencedirect.com/science/article/pii/S0306261917303495.

[10] Javaid N, Naseem M, Rasheed MB, Mahmood D, Khan SA, Alrajeh N, Iqbal Z. A new heuristically optimized home energy management controller for smart grid. Sustainable Cities Soc 2017;34:211–27. http://dx.doi.org/10.1016/j.scs.2017.06.009, URL https://www.sciencedirect.com/science/article/pii/S2210670717303074.

[11] Gazafroudi AS, Prieto-Castrillo F, Pinto T, Corchado JM. Energy flexibility management in power distribution systems: Decentralized approach. In: 2018 international conference on smart energy systems and technologies. SEST, 2018, p. 1–6. http://dx.doi.org/10.1109/SEST.2018.8495713.

[12] SoltaniNejad Farsangi A, Hadayeghparast S, Mehdinejad M, Shayanfar H. A novel stochastic energy management of a microgrid with various types of distributed energy resources in presence of demand response programs. Energy 2018;160:257–74. http://dx.doi.org/10.1016/j.energy.2018.06.136, URL https://www.sciencedirect.com/science/article/pii/S0360544218312015.

[13] Bendato I, Bonfiglio A, Brignone M, Delfino F, Pampararo F, Procopio R. A real-time energy management system for the integration of economical aspects and system operator requirements: Definition and validation. Renew Energy 2017;102:406–16. http://dx.doi.org/10.1016/j.renene.2016.10.061, URL https://www.sciencedirect.com/science/article/pii/S0960148116309387.

[14] Ahmed MS, Mohamed A, Khatib T, Shareef H, Homod RZ, Ali JA. Real time optimal schedule controller for home energy management system using new binary backtracking search algorithm. Energy Build 2017;138:215–27. http://dx.doi.org/10.1016/j.enbuild.2016.12.052, URL https://www.sciencedirect.com/science/article/pii/S0378778816313913.

[15] Forero-Quintero J-F, Villafáfila-Robles R, Barja-Martinez S, Munné-Collado I, Olivella-Rosell P, Montesinos-Miracle D. Profitability analysis on demand-side flexibility: A review. Renew Sustain Energy Rev 2022;169:112906. http://dx.doi.org/10.1016/j.rser.2022.112906, URL https://www.sciencedirect.com/science/article/pii/S1364032122007882.

[16] Menniti D, Sorrentino N, Pinnarelli A, Mendicino L, Brusco G, Vizza P, Graditi G. Management model of nanogrid based community energy storage. In: 2020 AEIT international annual conference. AEIT, 2020, p. 1–6. http://dx.doi.org/10.23919/AEIT50178.2020.9241164.

[17] Chen H, Xiong R, Lin C, Shen W. Model predictive control based real-time energy management for hybrid energy storage system. CSEE J Power Energy Syst 2021;7(4):862–74. http://dx.doi.org/10.17775/CSEEJPES.2020.02180.

[18] Elkazaz M, Sumner M, Thomas D. Real-time energy management for a small scale pv-battery microgrid: Modeling, design, and experimental verification. Energies 2019;12(14). http://dx.doi.org/10.3390/en12142712, URL https://www.mdpi.com/1996-1073/12/14/2712.

[19] Wu J, Wei Z, Li W, Wang Y, Li Y, Sauer DU. Battery thermal-and health-constrained energy management for hybrid electric bus based on soft actor-critic drl algorithm. IEEE Trans Ind Inf 2021;17:3751–61. http://dx.doi.org/10.1109/TII.2020.3014599.

[20] Chen H, Xiong R, Lin C, Shen W. Model predictive control based real-time energy management for hybrid energy storage system. CSEE J Power Energy Syst 2021;7:862–74. http://dx.doi.org/10.17775/CSEEJPES.2020.02180.

[21] Nemati M, Braun M, Tenbohlen S. Optimization of unit commitment and economic dispatch in microgrids based on genetic algorithm and mixed integer linear programming. Appl Energy 2018;210:944–63. http://dx.doi.org/10.1016/j.apenergy.2017.07.007, URL https://www.sciencedirect.com/science/article/pii/S0306261917308723.

[22] DataPort Data Base. Dataport data base. 2022, doi:https://dataport.cloud/. URL [Online;accessed07-September-2022].

[23] Wang Z, Wu W, Zhang B. A fully distributed power dispatch method for fast frequency recovery and minimal generation cost in autonomous microgrids. IEEE Trans Smart Grid 2016;7:19–31. http://dx.doi.org/10.1109/TSG.2015.2493638.

[24] Battke B, Schmidt TS, Grosspietsch D, Hoffmann VH. A review and probabilistic model of lifecycle costs of stationary batteries in multiple applications. Renew Sustain Energy Rev 2013;25:240–50. http://dx.doi.org/10.1016/j.rser.2013.04.023, cited by: 242. URL https://www.scopus.com/inward/record.uri?eid=2-s2.0-84878216650&doi=10.1016%2fj.rser.2013.04.023&partnerID=40&md5=6e2673fba9e07069ee80fbb9a7a25de9.

[25] Moreno-Bernal Pedro, Hernández-Callejo Luis, Nesmachnow Sergio, Rossit Diego, Correa Ochoa, Danny. Proceedings of the V Ibero-American congress of smart cities (ICSC-CITIES 2022). 2023.

[26] Farsangi AS, Hadayeghparast S, Mehdinejad M, Shayanfar H. A novel stochastic energy management of a microgrid with various types of distributed energy resources in presence of demand response programs. Energy 2018;160:257–74. http://dx.doi.org/10.1016/j.energy.2018.06.136.

[27] Nazari-Heris M, Abapour S, Mohammadi-Ivatloo B. Optimal economic dispatch of fc-chp based heat and power micro-grids. Appl Therm Eng 2017;114:756–69. http://dx.doi.org/10.1016/j.applthermaleng.2016.12.016.

[28] Samuel O, Javaid N, Khalid A, Khan WZ, Aalsalem MY, Afzal MK, Kim BS. Towards real-time energy management of multi-microgrid using a deep convolution neural network and cooperative game approach. IEEE Access 2020;8:161377–95. http://dx.doi.org/10.1109/ACCESS.2020.3021613.

[29] Xu T, Wu W, Zheng W, Sun H, Wang L. Fully distributed quasi-newton multi-area dynamic economic dispatch method for active distribution networks. IEEE Trans Power Syst 2018;33:4253–63. http://dx.doi.org/10.1109/TPWRS.2017.2771950.

[30] Mo X, Zhu J, Chen J, Guo Y, Xia Y, Liu M. A stochastic spatiotemporal decomposition decision-making approach for real-time dynamic energy management of multi-microgrids. IEEE Trans Sustain Energy 2021;12:821–33. http://dx.doi.org/10.1109/TSTE.2020.3021226.

[31] Warrington J, Mariéthoz S, Jones CN, Morari M. Predictive power dispatch through negotiated locational pricing. IEEE Computer Society; 2010, http://dx.doi.org/10.1109/ISGTEUROPE.2010.5638858.

[32] Jokic A, Bosch PPVD, Hermans RM. Distributed, price-based control approach to market-based operation of future power systems. 2009, http://dx.doi.org/10.1109/EEM.2009.5207170.

[33] Zahedmanesh A, Muttaqi KM, Islam MR, Zhao Y. Consensus-based decision making approach for techno- economic operation of largescale battery energy storage in industrial microgrids. J Energy Storage 2022;46. http://dx.doi.org/10.1016/j.est.2021.103917.